HHS Public Access

Author manuscript

Mol Psychiatry. Author manuscript; available in PMC 2015 August 01.

Published in final edited form as:

Mol Psychiatry. 2015 February ; 20(2): 162–169. doi:10.1038/mp.2014.143.

Functional implications of a psychiatric risk variant within *CACNA1C* in induced human neurons

Takao Yoshimizu[1,2,*], **Jen Q. Pan**[3,7,*], **Alison E. Mungenast**[1,2,&], **Jon M. Madison**[3,&], **Susan Su**[1,2], **Josh Ketterman**[3], **Dost Ongur**[4], **Donna McPhie**[4], **Bruce Cohen**[4], **Roy Perlis**[3,5], and **Li-Huei Tsai**[1,2,6,7]

[1]Picower Institute for Learning and Memory, Massachusetts Institute of Technology (MIT), Cambridge, Massachusetts, 02139

[2]Department of Brain and Cognitive Sciences, MIT, Cambridge, Massachusetts, 02139

[3]Stanley Center for Psychiatric Research, Broad Institute, Cambridge, MA 02142

[4]McLean Hospital and Department of Psychiatry, Harvard Medical School, Boston, Massachusetts, USA

[5]Bipolar Clinic and Research Program, Massachusetts General Hospital and Harvard Medical School, Boston, MA, 02114

[6]Howard Hughes Medical Institute, Massachusetts Institute of Technology, Cambridge, MA 02139

Abstract

Psychiatric disorders have clear heritable risk. Several large-scale genome-wide association studies have revealed a strong association between susceptibility for psychiatric disorders, including bipolar disease, schizophrenia, and major depression, and a haplotype located in an intronic region of the L-type voltage gated calcium channel (VGCC) subunit gene *CACNA1C* (peak associated SNP rs1006737), making it one of the most replicable and consistent associations in psychiatric genetics. In the current study, we used induced human neurons to reveal a functional phenotype associated with this psychiatric risk variant. We generated induced human neurons, or iN cells, from more than 20 individuals harboring homozygous risk genotypes, heterozygous, or homozygous non-risk genotypes at the rs1006737 locus. Using these iNs, we performed electrophysiology and quantitative PCR experiments that demonstrated increased L-type VGCC current density as well as increased mRNA expression of *CACNA1C* in induced neurons homozygous for the risk genotype, compared to non-risk genotypes. These studies demonstrate that the risk genotype at rs1006737 is associated with significant functional alterations in human

[7]To whom correspondence should be addressed: lhtsai@mit.edu; jpan@broadinstitute.org.

*,&These authors contributed equally

Author contributions

TY, JQP, AEM, JMM, and LHT conceived and designed the study; TY, JQP, JMM, AEM, and LHT wrote the manuscript; TY and JMM developed the iN protocol. TY conducted immunocytochemistry and qPCR; JQP and SS conducted electrophysiology, AEM conducted qPCR; TY, AEM, and JK created lentivirus and cultured iN cells; OD, DM, and JMM facilitated the collection of human fibroblasts; JMM confirmed the genotypes. RP and BC provided patient fibroblasts.

induced neurons, and may direct future efforts at developing novel therapeutics for the treatment of psychiatric disease.

Introduction

Severe neuropsychiatric disorders, such as schizophrenia and bipolar disease, have a substantial and consistently observed genetic component[1]. Unfortunately, the limitations of animal models for neuropsychiatric disease and the lack of human model systems has limited our ability to explore the relationship between the genomic determinants and the cellular and molecular biology abnormalities underlying these diseases in neural cells[2]. Genome-wide association studies (GWAS) using large psychiatric disorder cohorts have yielded reproducible common and rare genetic variations that are associated with disease risk, but the mechanistic roles of these risk genes in disease etiology and pathophysiology remain largely unknown.

Mutations in the *CACNA1C* gene have been associated with autism spectrum disorders (ASD) and, in at least one case, bipolar disorder symptoms[3]. In 2008, Ferriera et al confirmed that a common intronic risk haplotype within the *CACNA1C* gene (peak risk SNP rs1006737) is associated with bipolar disorder[4]. The risk haplotype resides within a 100kb segment of a large (300 kb) intron within the *CACNA1C* gene. Subsequently, it was shown that the same risk allele within *CACNA1C* also conferred risk for recurrent major depression and schizophrenia[5–7]. *CACNA1C* encodes the α_{1C} subunit ($Ca_V1.2$)[8], of the L-type voltage-gated calcium channel (VGCC), which activates upon cellular depolarization, and underlies key neuronal functions such as dendritic information integration, cell survival, and neuronal gene expression[9]. Human brain imaging and behavioral studies have demonstrated morphological and functional alterations in individuals carrying the *CACNA1C* risk allele[10–13]. However, no study has examined the cellular impact of the risk SNP in *CACNA1C* directly on channel function in human neurons.

The ability to proceed past the initial identification of risk variants and examine the biological consequences of disease-associated variants has been facilitated by recent developments in *in vitro* approaches that give researchers access to neural cell lines that carry the intact genome of affected individuals. Induced pluripotent stem cell (iPSC) technology has enabled studies to associate cellular phenotypes with a specific Timothy Syndrome mutation within the coding exon of *CACNA1C* using stem cell-derived neurons[14]. As an alternative to the iPSC approach, the technology of rapid neuronal programming, in which mouse or human fibroblasts are directly converted into functional induced neurons (iNs), can efficiently and rapidly produce functional human neurons[15, 16]. In the current report, the shorter induction protocol of the iN technique allowed us to rapidly derive human neuron-like cells from a relatively large library of fibroblasts obtained from individuals with and without the risk associated SNP at rs1006737, representing perhaps the largest cohort, to date, of re-programmed human neuronal cells. Using these cells, we evaluated the functional impact of the intronic risk haplotype at the rs1006737 SNP within the *CACNA1C* gene.

In the current work, we observed that *CACNA1C* mRNA was more abundant in iNs from individuals carrying the rs1006737 risk genotype, compared to those with the non-risk

genotype. Additionally, iNs carrying the risk SNP displayed higher L-type VGCC calcium current densities compared to iNs carrying the non-risk variant. These findings are the first to demonstrate a functional neuronal phenotype for a non-coding variant associated with psychiatric disease risk in induced neurons derived from patient and/or control subject fibroblasts, providing novel insights into the functional consequences of genetic variants associated with psychiatric disorders. We show that the direct reprogramming of human fibroblasts into neuronal cells represents a feasible means by which elements of these complex disorders may be investigated at the cellular and molecular level using neurons derived from groups of individuals carrying disease risk-associated SNPs.

Results

Human iN cells display neuronal phenotypes

We obtained human dermal fibroblasts (Supplementary Fig. 1a) and determined their genotypes for the *CACNA1C* SNP rs1006737 using PCR followed by Sanger sequencing (Supplementary Table 1). To generate induced neurons (iNs) from human fibroblasts, the human transcription factors *ASCL1*, *POU3F2*, and *MYT1L* cDNAs were individually cloned into lentiviral vectors preceding an IRES-EGFP cassette under the control of the CMV promoter (Fig. 1a). As early as one week following the lentiviral transduction of human fibroblasts, we observed neuron-like GFP-positive cells extending processes from large round soma in culture (Fig. 1b–f, h, and Supplementary Fig. 1b). Using immunocytochemical methods, we confirmed that these induced neurons expressed neuron-specific markers, such as Tuj1, MAP2, NeuN (Fig. 1b–d). When these iNs were transduced with a lentivirus expressing RFP from the human synapsin promoter we also observed co expression of RFP with these markers (Fig. 1e). In addition, human iNs co-cultured with human astrocytes for 28 days expressed immunoreactivity for the vesicular glutamate transporter VGLUT1 (Fig. 1f).

To further characterize the neuronal properties of these iN cells, we performed RT-PCR analysis and compared their expression of neuronal markers with the expression of these markers in normal human neural progenitor cells (hNPCs), differentiated hNPCs, and human whole brain mRNA. We found that the iNs did not express progenitor markers such as *SOX2* or *CUX2*, but instead expressed well-known neuronal markers including *MAP2*, *FOXP2*, *TBR1*, *GRIN1* (NR1), *GABRA6*, *GABRB2*, *NTRK2* (TrkB), and *SLC17A7* (VGLUT1). These data suggest that the iNs are terminally differentiated and are not self-replenishing. Interestingly, we did not observe *SLC32A1* (VGAT) mRNA in our iN cells, suggesting that these cells have a glutamatergic, rather than GABAergic, neuronal phenotype (Fig. 1g).

Membrane excitability is a functional hallmark of neurons. To determine if these iNs were electrically excitable, we performed electrophysiological recordings. We recorded from cells that exhibited both GFP fluorescence and typical neuronal morphologies, and found that the iN cells had average resting membrane potentials similar to those reported previously for directly induced neurons[15–17] (-51 mV, +/- 3.3 mV, n=6, 21 days post-transduction). In addition, step current injections ranging from −90 to +50 pA elicited action potentials from iN cells. These characteristics indicate that the iN cells were excitable, and thus displayed a functional neuronal phenotype (Fig. 1h). We successfully converted all the fibroblast lines

used in this study to iNs (Supplementary Fig. 1b) and found that, on average, more than 50% of the GFP-positive cells co-expressed the neuronal marker Tuj1 (data not shown).

Higher mRNA levels of CACNA1C expressed in iNs harboring the risk variant at rs1006737

To examine the functional relevance of a genomic variant associated with psychiatric disease, we obtained over 20 human fibroblast lines homozygous for the non-risk (GG, 9 lines), homozygous for the risk (AA, 12 lines), or heterozygous (GA, 3 lines) for the risk allele at rs1006737 within the *CACNA1C* gene and induced these fibroblasts to form iNs. We prioritized the collection of the two homozygous groups in this study, to better detect potential effects of this specific genomic variation in the context of a variety of human genomes. To measure expression levels of *CACNA1C* mRNA in these neurons, we designed primers that spanned exons 3 and 4 of *CACNA1C*, thus flanking the intronic rs1006763 SNP[18]. Using these primers, the *CACNA1C* amplicon derived from these neurons was cloned and subjected to Sanger sequencing to confirm its identity (data not shown). Three to four weeks following viral transduction, we used a micropipette to isolate 5 – 10 iN cells from each heterogeneous culture. We selected only those GFP-positive cells that displayed distinct neuronal morphologies and expressed exogenous RFP driven by the neuron-specific synapsin promoter (Fig. 1e). Using quantitative real-time PCR (qPCR), we discovered that iNs derived from individuals harboring the homozygous risk AA genotype on average expressed significantly higher levels of *CACNA1C* mRNA compared to cells harboring the non-risk GG or the heterozygous risk AG genotype (Fig. 2). These results suggest that the rs1006763 haplotype variations influenced the level of *CACNA1C* transcripts in these human neural cells.

L-type voltage-gated calcium channel (VGCC) currents are evident in induced neurons

To investigate whether L-type VGCC currents are present in iNs, whole-cell recordings were conducted prior to and following the neuronal induction protocol. As shown in Supplemental Figure 2a, little VGCC current was detected in primary human fibroblasts prior to induction. Two weeks following virus-mediated iN induction, inward calcium currents measured from GFP-positive iN cells with more than two processes could be evoked by step-wise depolarization from a holding potential of −100 to test potentials between −50 mV to +50 mV at 5 mV steps. The current density (peak current, pA normalized to cell capacitance, pF), measured from iNs derived from more than 20 human fibroblast lines, averaged 4.9 ± 0.2 pA/pF, (mean ± s.e.m., n = 305), using 10 mM Ba^{2+} as the charge carrier. iNs derived from fibroblasts of different human subjects demonstrated similar current-voltage relationship in activation (Supplemental Fig. 2b), with peak current elicited at +10 mV. Next, we examined the steady state inactivation (SSI) profile of VGCCs in these iNs. SSI is a measure of channel availability at a given holding potential. As shown in Supplemental Fig. 2c, VGCC currents in these iNs exhibited similar SSI profiles and the magnitude of $V_{1/2,inact}$, the membrane potential at which half of the channels are available to open (Supplemental Fig. 2c). Both voltage dependent activation and inactivation profiles of VGCC in iNs were consistent with canonical high-voltage gated calcium currents[19].

To dissect the components of the calcium currents recorded in these iNs, we applied pharmacological inhibitors of N- and P/Q type channels. Following the application of ω-

conotoxins GVIA and MVIIC (400 nM), which are specific N and P/Q type channel blockers[20, 21], respectively, to the recording solutions, we observed little reduction in the amplitude of the inward calcium current (data not shown). In contrast, the L-type VGGC blocker, nifedipine, dose dependently inhibited these iN calcium currents, reaching nearly complete block at 1 μM (Fig. 3a), while the L-type VGCC activator Bay K8840 (2 μM), potentiated the size of the iN dramatically (average fold of potentiation: 7.2 ± 1.7, n =3; mean ± s.e.m). We then examined the effects of another dihydropyridine L-type channel inhibitor, isradipine, on iN calcium currents, and found that the half maximal inhibitory concentration (IC_{50}) of isradipine on calcium currents is 33.1 ± 2.9 nM (Supplemental Fig. 2d) using iNs induced from subject GM03440, which was consistent with previous reports of L-type VGCC pharmacology[22]. Of note, isradipine has recently been reported to be efficacious in the treatment of bipolar depression[23].

Two genes, *CACNA1C* and *CACNA1D*, encode the α_1 subunits of the neuronal L-type calcium channel. The biophysical properties and pharmacological properties of these two VGCCs would be hard to distinguish under the recording conditions described herein. Therefore, we sought to determine by RT-PCR whether *CACNA1D* was also expressed in these iNs. We isolated total RNA from induced neurons and the subsequent RT-qPCR showed that transcripts for the closely-related *CACNA1D* gene were completely absent in the iN cells (Supplementary Fig. 2e). Additionally, transcripts for other calcium channel genes such as *CACNA1B, CACNA1E,* and *CACNA1H* were also absent. Interestingly, although we do not detect P/Q-mediated currents, mRNA transcripts for the *CACNA1A* gene were detectable in the iN cells using RT-qPCR (data not shown). These data collectively suggest the VGCC currents recorded from iNs result primarily from L-type channels containing the α_{1C} subunit expressed from the *CACNA1C* gene.

Human induced neurons carrying the risk CACNA1C SNP exhibit an enhanced calcium current density

To address whether the rs1006763 risk haplotype influences the properties of L-type VGCC currents in induced neurons, we performed electrophysiological recordings on the iNs derived from individuals with different genotypes at rs1006763. Strikingly, we found that the calcium current density from different iN cell lines was significantly different among the iNs from different genotypes (risk vs. non-risk), while the voltage-dependence of activation was similar across all cell lines (Fig. 3b). The VGCC current density overall was significantly higher in iNs derived from subjects with the risk (AA) rs1006763 genotype compared to iNs derived from those who harbored heterozygous or homozygous non-risk genotype (GA or GG; Fig. 3c, 3d). We also show that, overall, the current densities of these cell lines were correlated with the qPCR quantification of *CACNA1C* mRNA (R = 0.65; Fig. 3e). While the averaged current density significantly differed among genotypes (Fig. 3c), the average size of the iN cells, as measured by cell capacitance, was not significantly different (AA: 18.4 ± 8.2, pF, n= 132; GA: 20.0 ± 7.7 pF, n = 58; GG: 20.1±8.6 pF, n= 115; mean ± s.d.). Not all lines that had a risk genotype showed increased current density and *CACNA1C* expression, nor did all low-risk genotypes have lower current density and *CACNA1C* expression. For example, iNs derived from the ML-0673-01 homozygous risk (AA) line showed lower current densities and *CACNA1C* expression than the other risk cell lines. By

contrast, the homozygous non-risk (GG) line GM02036 displayed increased current densities, but similar *CACNA1C* expression, compared to other non-risk lines (Fig. 3c). Variation in other cellular factors, such as channel trafficking efficiency or auxiliary subunit expression levels, may account for these discrepancies by, for example, contributing to differences in channel plasma membrane surface densities without modifying the mRNA level of *CACNA1C*.

To confirm that the observed differences in current density were not the result of differences between induction batches, we analyzed VGCC currents from three independent inductions of two fibroblast cell lines. We found that iNs derived from the GM03440 line consistently produced higher averaged current densities (8.9 ± 3.0, 4.6 ± 0.8, and 8.3 ± 1.1 pA/pF) in three inductions, compared to those from GM05934 (2.8 ± 0.1, 1.4 ± 0.2, and 2.9 ± 0.5 pA/pF respectively) over the same induction batches (Supplemental Fig. 3f). These results indicate that the measurement of VGCC current density in iNs reflects a relatively stable property of these cells, one which is moderated mostly by specific genetic variation in the fibroblast donors, rather than resulting from subtle differences in conditions during induction. Together with our RT-qPCR data from isolated neurons, these electrophysiological data suggest that the presence of the psychiatric risk genotype (peak SNP rs1006763) increases *CACNA1C* transcription in excitatory induced human neurons. Moreover, this alteration in *CACNA1C* expression is associated with increased L-type VGCC current density in these cells.

Discussion

Our study represents the first attempt, to our knowledge, to examine a genetic risk factor comprised of a common illness related common variant in human induced neurons. We demonstrate, at single-neuron resolution, that a non-coding psychiatric risk genotype can influence the physiological function of human neural cells. Our findings support the use of human-derived neurons in the study of neurological disease mechanisms and their utility for potential therapeutic target identification. In the current report, we directly reprogrammed 24 human fibroblast lines into iN cells to study the effects of rs1006737 risk and non-risk haplotypes in human-derived neurons. We showed that the risk rs1006737 genotype (AA) is correlated with increased levels of *CACNA1C* mRNA as compared to the non-risk or heterozygous (GG, GA) genotypes in iNs. Importantly, we found a functional difference between risk and non-risk genotype neurons, namely, an increase in the density of $Ca_V1.2$-mediated currents in iNs harboring the risk genotype, compared to the non-risk genotype. As cells carrying the risk allele at rs1006737 were obtained from both healthy individuals and psychiatric patients (Supplemental Table 1), the current study examines the functional impact of this genetic variant independent of psychiatric diagnosis. These results support the notion that variations at the rs1006737 SNP in the *CACNA1C* gene are associated with $Ca_V1.2$ channel function in human excitatory neuron-like cells.

Interestingly, the presence of the rs1006763 risk haplotype has been associated with altered *CACNA1C* mRNA levels in postmortem human brain samples. One study showed that an increase in *CACNA1C* mRNA levels was associated with the risk haplotype[10]. In contrast, a recent work found that the risk haplotype at rs1006737 was associated with decreased

expression of *CACNA1C* in post-mortem human cerebellum[3]; however, no difference was found in the parietal cortex, suggesting that alternation in *CACNA1C* expression associated with this risk haplotype may be brain-region specific, as well as neuron subtype specific. In addition, while the current study examined only induced neurons, *CACNA1C* may be expressed in glial cells, such as astrocytes[24, 25]. In mature neurons, other calcium channel subunits are likely to be functional, such as P/Q channels encoded by the *CACNA1A* gene[26]. In the iN cells, however, although mRNA is evident for *CACNA1A*, our electrophysiological findings indicate that this channel did not contribute significantly to recorded total whole cell calcium currents 2 weeks post transduction. Thus, our results cannot yet be compared directly to post mortem findings. We speculate that the large intronic region, where the disease risk associated variants resides, regulates *CACNA1C* expression through multiple cis-elements and that these cis-elements are active in different types of cells and at different developmental stages. Future expression analysis in single primary neurons, rapidly-reprogrammed neurons of different subtypes[27], or isolated neural populations from different regions of human brain, will be necessary to determine the potential regional and cell-type specific impact of this risk haplotype on calcium channel gene expression.

It is important to note that two of the 24 cell lines analyzed showed a phenotype discordant from that of the rest of their group. In one line, ML-0673-01, homozygous for the risk genotype, we observed lower *CACNA1C* mRNA levels and lower VGCC-mediated current density. Another line, GM02036, which was homozygous for the non-risk genotype, displayed increased current densities, although *CACNA1C* mRNA levels were similar to the rest of the non-risk group. These data suggest that, while the haplotype at rs1006737 may be a significant contributing factor in influencing L-type VGCC expression and function in these human neurons, other genomic variation may also play a role. This incompletely penetrant pattern becomes apparent after analyzing a sizable pool of reprogrammed cell lines. Future studies using genome-editing technologies, such as TALEN or CRISPR[28–32], to generate isogenic genomes that differ only at causal variations in this region could reveal the functional impact of this risk SNP in the absence of other genome variability.

The use of a renewable source of patient and unaffected human neurons to demonstrate a specific neuronal function is altered by a psychiatric risk haplotype is a milestone in the field of psychiatric biology. Several previous pharmacological studies have implicated the L-type VGCC in psychiatric disease. L-type calcium currents are down-regulated in the mouse brain in response to antipsychotics, and calcium channel antagonists, such as verapamil and isradipine, have been used therapeutically in bipolar disease treatment[33–35]. In addition, recent studies have shown an impact of the rs1006737 *CACNA1C* haplotype in task-based human behaviors, such as spatial working memory and attention, as well as on morphological changes such as grey matter volume of specific regions of human brain[10–12, 36–40]. The current study suggests a potential strategy with which to study these psychiatric disorders at the molecular and cellular level, a strategy that may help prioritize experiments for the downstream identification and validation of psychiatric risk genes, and impact the development of novel therapeutic approaches for these common disorders.

Methods

Molecular cloning and lentivirus production

Human *ASCL1*, *POU3F2*, and *MYT1L* cDNAs were separately cloned into lentiviral vector pHRST-IRES-EGFP, containing an IRES-EGFP cassette under the control of a CMV promoter. The human synapsin I promoter driving DsRed in a lentiviral plasmid (Addgene Plasmid 22909: pLV-hSyn-RFP) was obtained from Addgene. VSV-G-coated lentiviral particles were packaged in 293T cells as described previously[41]. Briefly, 293T cells were transfected with each lentiviral plasmid coding for human *ASCL1*, *POU3F2*, or *MYT1L* and envelope plasmids (Addgene Plasmids 12259: pMD.2G and 12263: pCMVdeltaR8.2) using Lipofectamine 2000 (Invitrogen). The medium was replaced 6-10 hours after the transfection, and the supernatant containing the viruses was then harvested at 72 hours post transfection, filtered, and ultracentrifuged to concentrate the virus. Aliquots of the viruses were stored at −80 °C until use.

Cell culture

Human fibroblasts were obtained from the Coriell Institute, McLean Hospital, Massachusetts General Hospital, and the *American Type Culture Collection* (ATCC). Human fibroblasts were cultured in D15 media (DMEM containing GlutaMAX (Invitrogen), 15% FBS and penicillin/streptomycin). These fibroblasts were genotyped by droplet digital PCR at the Broad Institute. The 293T cells for lentivirus production were grown in D10 media (DMEM containing GlutaMAX and 10% FBS). Human normal neuronal progenitor cells (NPCs) were obtained from Massachusetts General Hospital, and were cultured in NPC media (70% DMEM/30% F12 containing GlutaMAX, B27 supplement (Invitrogen), 20 ng/ml FGF2 (R&D Systems), 20 ng/ml EGF (R&D Systems) and 5μg/ml heparin (Sigma). For the differentiation of NPCs, cells were cultured in 70% DMEM/30% F12 medium containing B27 supplement without FGF2, EGF, and heparin for 6-8 weeks. To generate human iNs, human fibroblasts were plated onto dishes or glass coverslips treated with poly-D-lysine/laminin at appropriate cell densities and the next day were transduced with lentiviruses carrying the three iN factors in D15 media containing 8 μg/ml polybrene. After 6-12 hours in the transduction medium, the cells were switched to N3 medium (DMEM/F12 containing GlutaMAX, 25 μg/ml insulin (Sigma), 30 nM sodium selenite (Sigma), 20 nM progesterone (Sigma), 100 nM putrescine (Sigma), 50 μg/ml transferrin (Roche Applied Science), and 10 ng/ml FGF2 for the conversion into iNs. For long-term iN culture, 10 ng/ml BDNF (R&D systems) was added to the medium after the third week of induction. The medium was replaced every few days for the duration of the culture period. Normal human astrocytes were obtained from Lonza and cultured in Astrocyte Basal Medium (Lonza). For co-culturing with human astrocytes, iNs were dissociated with Accutase (Invitrogen) 4–6 days after viral transduction and replated onto monolayer cultures of human astrocytes. Human iNs co-cultured with human astrocytes were fed with N3 medium containing 10 ng/ml FGF2 and BDNF.

Immunofluorescence

For immunofluorescence labeling, cells were washed with PBS and then fixed with 4% paraformaldehyde for 10 min at room temperature. Following incubation in 0.1 M

glycine/PBS for 3 min and washing with PBS, cells were incubated in PBS containing 0.25% Triton X-100 (Sigma) and 10% normal donkey serum (Millipore) for 2 hours at room temperature. Primary antibody incubations were conducted overnight at 4 °C. Following three PBS washes, cells were incubated with appropriate secondary antibodies for 1 hour at room temperature, followed by three PBS washes. All primary and secondary antibodies were diluted in a solution of PBS containing 10% normal donkey serum. Slides were mounted with Vectashield containing 1.5 μg/ml DAPI (4′,6-diamidino-2-phenylindole) to visualize nuclei. Images were acquired using a Zeiss LSM 510 confocal microscope. The following primary antibodies were used for the present study: mouse anti-Tuj1 (Covance, 1:2,000), mouse anti-MAP2 (Sigma, 1:2,000), mouse anti-NeuN (Millipore, 1:200), rabbit anti-VGLUT1 (Synaptic Systems, 1:5,000). DyLight488-, DyLight549- and Cy3-conjugated donkey secondary antibodies were obtained from Jackson ImmunoResearch and all were used at 1:2,000.

RT-PCR and quantitative (q)RT-PCR

For RT-PCR, total RNA was isolated from human fibroblasts, day 28 iNs, and normal human NPCs using the RNeasy Plus kit (Invitrogen) following the manufacturer's instructions. cDNAs were synthesized with using Superscript III (Invitrogen) with oligo(dT) and random hexamers. Human whole brain cDNA was obtained from Clontech. PCR products, amplified using each gene-specific primer set, were analyzed on 2% agarose gels. For isolated cell-based qRT-PCR, ~10 GFP-positive iNs that co-expressed DsRed driven by the neuron-specific synapsin promoter were collected by aspiration into patch electrodes with 10 mM HEPES buffer (pH 7.4) containing 150 mM NaCl, 5 mM KCl, 2.4 mM $CaCl_2$, 1.3 mM $MgCl_2$, and 10 mM glucose. Cells were also selected based on their neuron-like morphology, which included elevated, phase-bright cell bodies and the presence of multiple neurites. Selected iNs were then were ejected into tubes containing cell-collection buffer (10% iScript RT-qPCR Sample Preparation Reagent and RNase inhibitor) and rapidly frozen on dry ice. Cells were collected 21–28 days following induction. For analysis, samples were thawed on ice and subjected to reverse-transcription using the iScript cDNA Synthesis kit (Bio-Rad). Quantitative PCR was performed using SsoFast EvaGreen Supermix and the CFX96 Real-Time PCR Detection System (Bio-Rad). Results were compared with a standard curve generated by serial dilutions of input DNA. Primers used are listed in Supplementary Table 2 and normalized to GAPDH expression. For RT-PCR with whole cultures of iNs, cell lysates were prepared using iScript RT-qPCR Sample Preparation Reagent (Bio-Rad) following the manufacturer's instructions and were stored at −80 °C until use.

Electrophysiology

For electrophysiological recordings, cells were grown on 18 mm glass coverslips and transferred to a 35 mm dish containing the extracellular solution recording medium (140 mM TEA-Cl, 10 mM $BaCl_2$, 1 mM $MgCl_2$, 10 mM glucose, and 10 mM HEPES (pH 7.35, 325 mOsm). For calcium current recordings, patch pipettes were filled with the intracellular solution (125 mM CsCl, 4 mM $MgCl_2$, 4 mM Mg-ATP, 10 mM HEPES, 10 mM EGTA, and 1 mM EDTA (pH 7.2 with TEA-OH)). For action potential and K^+ or Na^+ channel recordings, the solutions were as follows; external solution: 130 mM NaCl, 4 mM KCl, 2

mM $CaCl_2$, 1 mM $MgCl_2$, 10 mM HEPES, and 10 mM glucose (pH 7.35, 325 mOsm); intracellular solution: 110 mM potassium gluconate, 20 mM KCl, 2 mM Mg-ATP, 10 mM sodium phosphocreatine, 1 mM EGTA, 0.3 mM GTP-Tris, and 20 mM HEPES (pH 7.25, 320 mOsm). Electrodes were fabricated from borosilicate capillary glass tubing (Warner Instruments) with a capillary glass puller (Sutter Instruments). The patch electrodes were fire-polished on a microforge (Narishige) and had resistances of 3–5 MΩ. After establishing whole-cell mode recordings, the cell membrane capacitance and series resistance were compensated to 75% electronically using a patch clamp amplifier (Axopatch 200B; Molecular Devices). Current protocol generation and data acquisition were performed using pClamp10 software on an IBM computer equipped with an analog-to-digital converter (Digidata 1440A; Axon Instruments). Calcium currents were measured by depolarizing voltage steps conducted from −50 mV to +50 mV in 5 mV steps across a 100 ms interval. The resulting current amplitude traces were plotted in a current-voltage (I/V) curve, where the X-axis demonstrates the voltage at which the current density (pA/pF) is measured (Y-axis). Current density is obtained when calcium current (pA) is divided by the cell capacitance, a proxy for the cell size (pF). Representative Ca_V currents in iNs from a number of individuals were measured using whole-cell recordings. The voltage dependence of activation did not differ among cell lines. Action potentials were elicited from iNs at various time-points following induction. Recordings were conducted on days 14, 16, 18, and 20 post-induction, based on the neuron-like morphology and high levels of GFP expression of the iN cells. Once the current-clamp mode was obtained, cells were maintained at a potential of approximately −65 to −70 mV. Step current injection protocols were used from −90 to +50 pA. We conducted measurements of membrane properties in iN cells at various time-points after induction. These included properties such as the action potential height, membrane capacitance, membrane input resistance, and resting membrane potential. Inward sodium current and outward potassium current were measured in voltage-clamp mode with voltage step protocols from −50 to +50 mV.

Supplementary Material

Refer to Web version on PubMed Central for supplementary material.

Acknowledgments

This work was supported by grants from the National Institutes of Health (R01-MH091115, RF1-AG042978, R01-NS051874 and R01-NS078839 to LHT; MH09395 and MH10028 to RP; R21MH099448-01 to JQP), and the Stanley Medical Research Institute (to LHT, JQP, and JMM).

References

1. Visscher PM, Goddard ME, Derks EM, Wray NR. Evidence-based psychiatric genetics, AKA the false dichotomy between common and rare variant hypotheses. Mol Psychiatry. 2012; 17(5):474–485. [PubMed: 21670730]
2. McCarroll SA, Hyman SE. Progress in the genetics of polygenic brain disorders: significant new challenges for neurobiology. Neuron. 2013; 80(3):578–587. [PubMed: 24183011]
3. Gershon ES, Grennan K, Busnello J, Badner JA, Ovsiew F, Memon S, Alliey-Rodriguez N, Cooper J, Romanos B, Liu C. A rare mutation of CACNA1C in a patient with bipolar disorder, and decreased gene expression associated with a bipolar-associated common SNP of CACNA1C in brain. Mol Psychiatry. 2013

4. Ferreira MA, O'Donovan MC, Meng YA, Jones IR, Ruderfer DM, Jones L, Fan J, Kirov G, Perlis RH, Green EK, Smoller JW, Grozeva D, Stone J, Nikolov I, Chambert K, Hamshere ML, Nimgaonkar VL, Moskvina V, Thase ME, Caesar S, Sachs GS, Franklin J, Gordon-Smith K, Ardlie KG, Gabriel SB, Fraser C, Blumenstiel B, Defelice M, Breen G, Gill M, Morris DW, Elkin A, Muir WJ, McGhee KA, Williamson R, MacIntyre DJ, MacLean AW, St CD, Robinson M, Van Beck M, Pereira AC, Kandaswamy R, McQuillin A, Collier DA, Bass NJ, Young AH, Lawrence J, Ferrier IN, Anjorin A, Farmer A, Curtis D, Scolnick EM, McGuffin P, Daly MJ, Corvin AP, Holmans PA, Blackwood DH, Gurling HM, Owen MJ, Purcell SM, Sklar P, Craddock N. Collaborative genome-wide association analysis supports a role for ANK3 and CACNA1C in bipolar disorder. Nat Genet. 2008; 40(9):1056–1058. [PubMed: 18711365]
5. Green EK, Grozeva D, Jones I, Jones L, Kirov G, Caesar S, Gordon-Smith K, Fraser C, Forty L, Russell E, Hamshere ML, Moskvina V, Nikolov I, Farmer A, McGuffin P, Holmans PA, Owen MJ, O'Donovan MC, Craddock N. The bipolar disorder risk allele at CACNA1C also confers risk of recurrent major depression and of schizophrenia. Mol Psychiatry. 2010; 15(10):1016–1022. [PubMed: 19621016]
6. Nyegaard M, Demontis D, Foldager L, Hedemand A, Flint TJ, Sorensen KM, Andersen PS, Nordentoft M, Werge T, Pedersen CB, Hougaard DM, Mortensen PB, Mors O, Borglum AD. CACNA1C (rs1006737) is associated with schizophrenia. Mol Psychiatry. 2010; 15(2):119–121. [PubMed: 20098439]
7. Moskvina V, Craddock N, Holmans P, Nikolov I, Pahwa JS, Green E, Owen MJ, O'Donovan MC. Gene-wide analyses of genome-wide association data sets: evidence for multiple common risk alleles for schizophrenia and bipolar disorder and for overlap in genetic risk. Mol Psychiatry. 2009; 14(3):252–260. [PubMed: 19065143]
8. Catterall WA, Perez-Reyes E, Snutch TP, Striessnig J. International Union of Pharmacology. XLVIII. Nomenclature and structure-function relationships of voltage-gated calcium channels. Pharmacological Reviews. 2005; 57(4):411–425. [PubMed: 16382099]
9. Greer PL, Greenberg ME. From synapse to nucleus: calcium-dependent gene transcription in the control of synapse development and function. Neuron. 2008; 59(6):846–860. [PubMed: 18817726]
10. Bigos KL, Mattay VS, Callicott JH, Straub RE, Vakkalanka R, Kolachana B, Hyde TM, Lipska BK, Kleinman JE, Weinberger DR. Genetic variation in CACNA1C affects brain circuitries related to mental illness. Arch Gen Psychiatry. 2010; 67(9):939–945. [PubMed: 20819988]
11. Franke B, Vasquez AA, Veltman JA, Brunner HG, Rijpkema M, Fernandez G. Genetic variation in CACNA1C, a gene associated with bipolar disorder, influences brainstem rather than gray matter volume in healthy individuals. Biol Psychiatry. 2010; 68(6):586–588. [PubMed: 20638048]
12. Zhang Q, Shen Q, Xu Z, Chen M, Cheng L, Zhai J, Gu H, Bao X, Chen X, Wang K, Deng X, Ji F, Liu C, Li J, Dong Q, Chen C. The Effects of CACNA1C Gene Polymorphism on Spatial Working Memory in Both Healthy Controls and Patients with Schizophrenia or Bipolar Disorder. Neuropsychopharmacology. 2011
13. Tesli M, Skatun KC, Ousdal OT, Brown AA, Thoresen C, Agartz I, Melle I, Djurovic S, Jensen J, Andreassen OA. CACNA1C risk variant and amygdala activity in bipolar disorder, schizophrenia and healthy controls. PLoS One. 2013; 8(2):e56970. [PubMed: 23437284]
14. Paşca SP, Portmann T, Voineagu I, Yazawa M, Shcheglovitov A, Paşca AM, Cord B, Palmer TD, Chikahisa S, Nishino S, Bernstein JA, Hallmayer J, Geschwind DH, Dolmetsch RE. Using iPSC-derived neurons to uncover cellular phenotypes associated with Timothy syndrome. Nature Medicine. 2011; 17(12):1657–1662.
15. Pang ZP, Yang N, Vierbuchen T, Ostermeier A, Fuentes DR, Yang TQ, Citri A, Sebastiano V, Marro S, Sudhof TC, Wernig M. Induction of human neuronal cells by defined transcription factors. Nature. 2011; 476(7359):220–223. [PubMed: 21617644]
16. Vierbuchen T, Ostermeier A, Pang ZP, Kokubu Y, Sudhof TC, Wernig M. Direct conversion of fibroblasts to functional neurons by defined factors. Nature. 2010; 463(7284):1035–1041. [PubMed: 20107439]
17. Pfisterer U, Kirkeby A, Torper O, Wood J, Nelander J, Dufour A, Bjorklund A, Lindvall O, Jakobsson J, Parmar M. Direct conversion of human fibroblasts to dopaminergic neurons. Proc Natl Acad Sci U S A. 2011; 108(25):10343–10348. [PubMed: 21646515]

18. Purcell SM, Wray NR, Stone JL, Visscher PM, O'Donovan MC, Sullivan PF, Sklar P, Ruderfer DM, McQuillin A, Morris DW, O'Dushlaine CT, Corvin A, Holmans PA, Macgregor S, Gurling H, Blackwood DHR, Craddock NJ, Gill M, Hultman CM, Kirov GK, Lichtenstein P, Muir WJ, Owen MJ, Pato CN, Scolnick EM, St Clair D, Williams NM, Georgieva L, Nikolov I, Norton N, Williams H, Toncheva D, Milanova V, Thelander EF, Sullivan P, Kenny E, Quinn EM, Choudhury K, Datta S, Pimm J, Thirumalai S, Puri V, Krasucki R, Lawrence J, Quested D, Bass N, Crombie C, Fraser G, Kuan SL, Walker N, McGhee KA, Pickard B, Malloy P, Maclean AW, Van Beck M, Pato MT, Medeiros H, Middleton F, Carvalho C, Morley C, Fanous A, Conti D, Knowles JA, Ferreira CP, Macedo A, Azevedo MH, Kirby AN, Ferreira MAR, Daly MJ, Chambert K, Kuruvilla F, Gabriel SB, Ardlie K, Moran JL. Common polygenic variation contributes to risk of schizophrenia and bipolar disorder. Nature. 2009; 460(7256):748–752. [PubMed: 19571811]

19. Brunet S, Scheuer T, Catterall WA. Cooperative regulation of Ca(v)1. 2 channels by intracellular Mg(2+), the proximal C-terminal EF-hand, and the distal C-terminal domain. J Gen Physiol. 2009; 134(2):81–94. [PubMed: 19596806]

20. Kim JI, Takahashi M, Martin-Moutot N, Seagar MJ, Ohtake A, Sato K. Tyr13 is essential for the binding of omega-conotoxin MVIIC to the P/Q-type calcium channel. Biochem Biophys Res Commun. 1995; 214(2):305–309. [PubMed: 7677735]

21. Boland LM, Morrill JA, Bean BP. omega-Conotoxin block of N-type calcium channels in frog and rat sympathetic neurons. J Neurosci. 1994; 14(8):5011–5027. [PubMed: 8046465]

22. Handrock R, Rao-Schymanski R, Klugbauer N, Hofmann F, Herzig S. Dihydropyridine enantiomers block recombinant L-type Ca2+ channels by two different mechanisms. J Physiol. 1999; 521(Pt 1):31–42. [PubMed: 10562332]

23. Ostacher MJ, Iosifescu DV, Hay A, Blumenthal SR, Sklar P, Perlis RH. Pilot investigation of isradipine in the treatment of bipolar depression motivated by genome-wide association. Bipolar Disord. 2013

24. Latour I, Hamid J, Beedle AM, Zamponi GW, Macvicar BA. Expression of voltage-gated Ca2+ channel subtypes in cultured astrocytes. Glia. 2003; 41(4):347–353. [PubMed: 12555202]

25. D'Ascenzo M, Vairano M, Andreassi C, Navarra P, Azzena GB, Grassi C. Electrophysiological and molecular evidence of L-(Cav1), N- (Cav2.2), and R- (Cav2. 3) type Ca2+ channels in rat cortical astrocytes. Glia. 2004; 45(4):354–363. [PubMed: 14966867]

26. Blalock EM, Porter NM, Landfield PW. Decreased G-protein-mediated regulation and shift in calcium channel types with age in hippocampal cultures. J Neurosci. 1999; 19(19):8674–8684. [PubMed: 10493768]

27. Zhang Y, Pak C, Han Y, Ahlenius H, Zhang Z, Chanda S, Marro S, Patzke C, Acuna C, Covy J, Xu W, Yang N, Danko T, Chen L, Wernig M, Südhof TC. Rapid Single-Step Induction of Functional Neurons from Human Pluripotent Stem Cells. Neuron. 2013; 78(5):785–798. [PubMed: 23764284]

28. Jiang W, Bikard D, Cox D, Zhang F, Marraffini LA. RNA-guided editing of bacterial genomes using CRISPR-Cas systems. Nat Biotech. 2013; 31(3):233–239.

29. Wang H, Yang H, Shivalila Chikdu S, Dawlaty Meelad M, Cheng Albert W, Zhang F, Jaenisch R. One-Step Generation of Mice Carrying Mutations in Multiple Genes by CRISPR/Cas-Mediated Genome Engineering. Cell. 2013; 153(4):910–918. [PubMed: 23643243]

30. Cong L, Ran FA, Cox D, Lin SL, Barretto R, Habib N, Hsu PD, Wu XB, Jiang WY, Marraffini LA, Zhang F. Multiplex Genome Engineering Using CRISPR/Cas Systems. Science. 2013; 339(6121):819–823. [PubMed: 23287718]

31. Hockemeyer D, Wang H, Kiani S, Lai CS, Gao Q, Cassady JP, Cost GJ, Zhang L, Santiago Y, Miller JC, Zeitler B, Cherone JM, Meng X, Hinkley SJ, Rebar EJ, Gregory PD, Urnov FD, Jaenisch R. Genetic engineering of human pluripotent cells using TALE nucleases. Nat Biotech. 2011; 29(8):731–734.

32. Miller JC, Tan S, Qiao G, Barlow KA, Wang J, Xia DF, Meng X, Paschon DE, Leung E, Hinkley SJ, Dulay GP, Hua KL, Ankoudinova I, Cost GJ, Urnov FD, Zhang HS, Holmes MC, Zhang L, Gregory PD, Rebar EJ. A TALE nuclease architecture for efficient genome editing. Nature Biotechnology. 2010; 29(2):143–148.

33. Levy NA, Janicak PG. Calcium channel antagonists for the treatment of bipolar disorder. Bipolar Disord. 2000; 2(2):108–119. [PubMed: 11252650]
34. Keers R, Farmer AE, Aitchison KJ. Extracting a needle from a haystack: reanalysis of whole genome data reveals a readily translatable finding. Psychological medicine. 2009; 39(8):1231–1235. [PubMed: 19215628]
35. Dunn RT, Frye MS, Kimbrell TA, Denicoff KD, Leverich GS, Post RM. The efficacy and use of anticonvulsants in mood disorders. Clin Neuropharmacol. 1998; 21(4):215–235. [PubMed: 9704164]
36. Wang F, McIntosh AM, He Y, Gelernter J, Blumberg HP. The association of genetic variation in CACNA1C with structure and function of a frontotemporal system. Bipolar disorders. 2011; 13(7–8):696–700. [PubMed: 22085483]
37. Roussos P, Giakoumaki SG, Georgakopoulos A, Robakis NK, Bitsios P. The CACNA1C and ANK3 risk alleles impact on affective personality traits and startle reactivity but not on cognition or gating in healthy males. Bipolar Disord. 2011; 13(3):250–259. [PubMed: 21676128]
38. Perrier E, Pompei F, Ruberto G, Vassos E, Collier D, Frangou S. Initial evidence for the role of CACNA1C on subcortical brain morphology in patients with bipolar disorder. European psychiatry : the journal of the Association of European Psychiatrists. 2011; 26(3):135–137. [PubMed: 21292451]
39. Thimm M, Kircher T, Kellermann T, Markov V, Krach S, Jansen A, Zerres K, Eggermann T, Stocker T, Shah NJ, Nothen MM, Rietschel M, Witt SH, Mathiak K, Krug A. Effects of a CACNA1C genotype on attention networks in healthy individuals. Psychological medicine. 2011; 41(7):1551–1561. [PubMed: 21078228]
40. Erk S, Meyer-Lindenberg A, Schnell K, Opitz von Boberfeld C, Esslinger C, Kirsch P, Grimm O, Arnold C, Haddad L, Witt SH, Cichon S, Nothen MM, Rietschel M, Walter H. Brain function in carriers of a genome-wide supported bipolar disorder variant. Arch Gen Psychiatry. 2010; 67(8):803–811. [PubMed: 20679588]
41. Soda T, Frank C, Ishizuka K, Baccarella A, Park YU, Flood Z, Park SK, Sawa A, Tsai LH. DISC1-ATF4 transcriptional repression complex: dual regulation of the cAMP-PDE4 cascade by DISC1. Mol Psychiatry. 2013

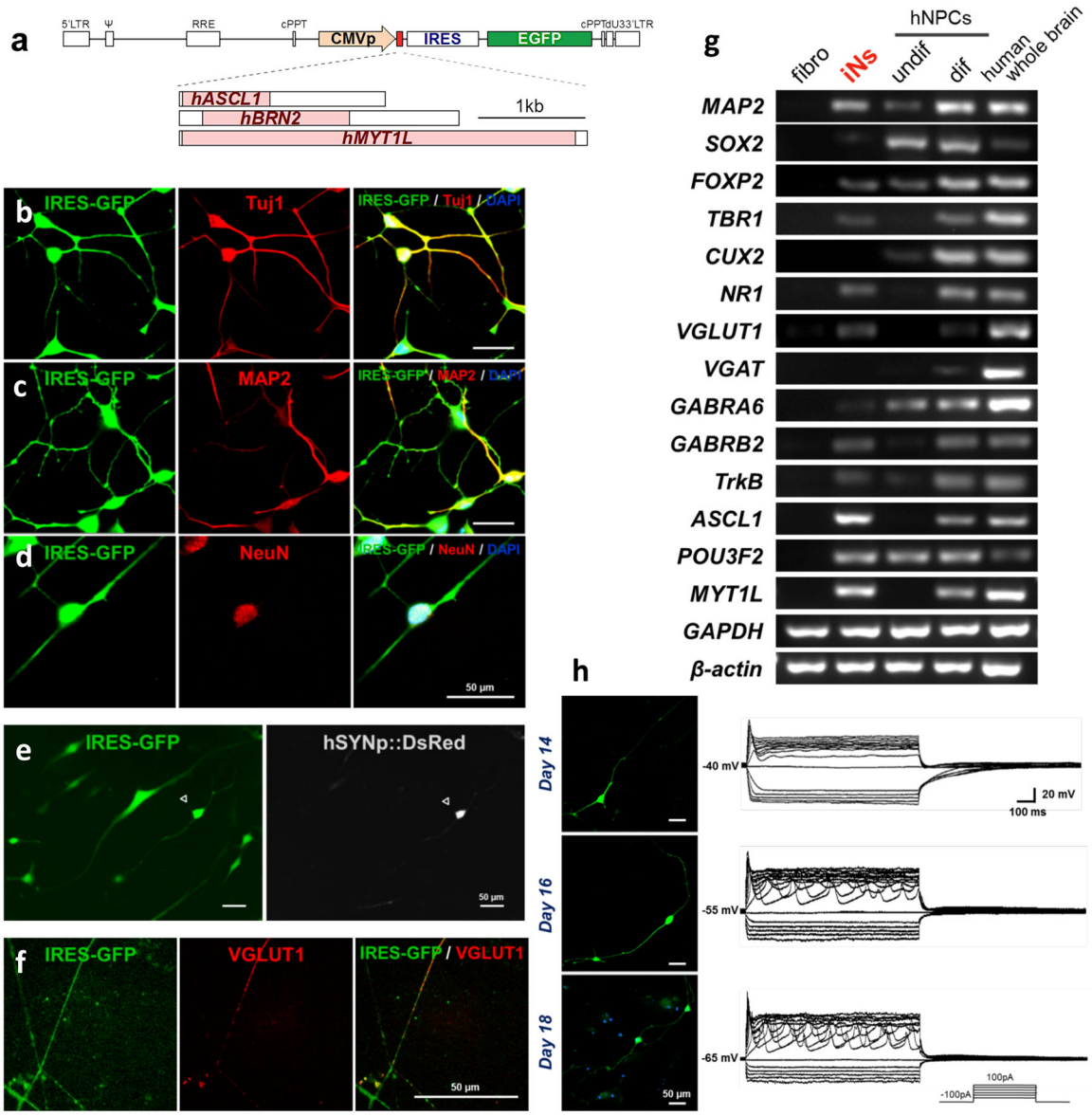

Figure 1. Human iN cells display neuronal phenotypes

a. Construction of lentivirus vectors for generating iNs from human fibroblasts. **b–e.** Human iNs have neuronal morphology and express several neuronal markers, Tuj1 (**b**), MAP2 (**c**), NeuN (**d**) and hSynapsin promoter driving DsRed (**e**) three weeks following induction. **f.** Human iNs co-cultured with human astrocytes express a presynaptic marker, VGLUT1. **g.** RT-PCR analyses reveal human iNs express neuronal markers including *FOXP2*, *TBR1*, *GRIN1(NR1)*, *GABRA6*, *GABRB2*, *NTRK2* (TrkB), and *SLC17A7 (VGLUT1)*, but not an inhibitory neuronal marker, *SLC32A1(VGAT)*. **h.** Representative traces showing action potentials with injected currents. Scale bars, 50 μm.

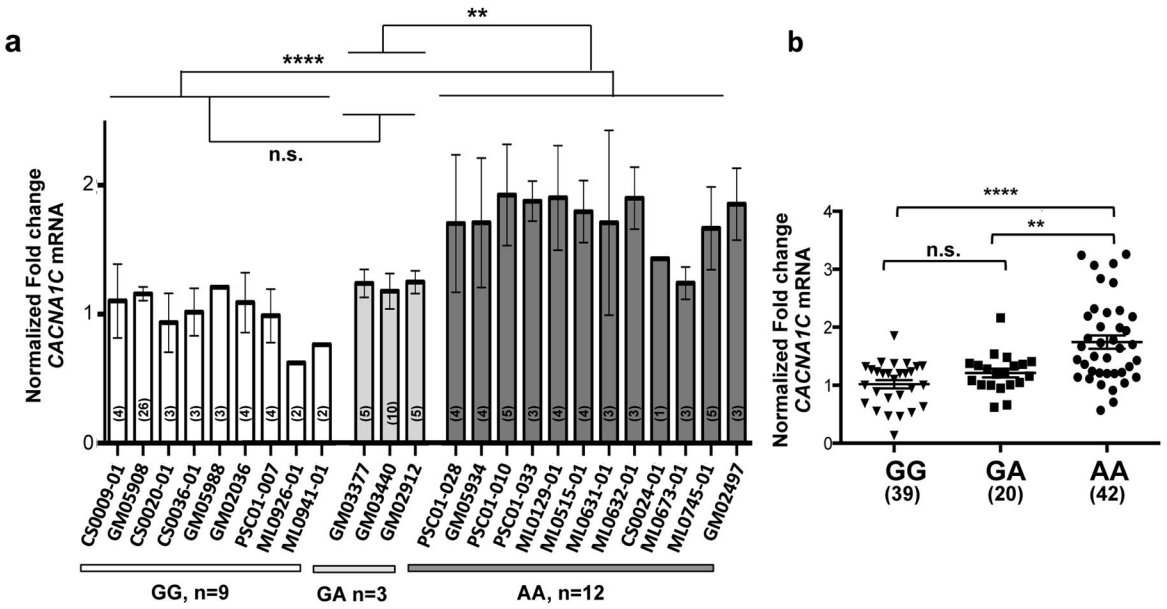

Figure 2. Quantification of *CACNA1C* mRNA levels in human iNs from different individuals using quantitative RT-PCR

(**a**) Histogram representing the fold changes in *CACNA1C* mRNA expression compared to the reference cell line GM05908. Each number within the column represents one qPCR experiment (~10 cells) for that line, normalized to *GAPDH* expression. Differences between cell line means were assessed using a one-way ANOVA ($F = 39.77$, $p < 0.0001$) with post-hoc Tukey's multiple comparisons test. GG = non-risk genotype, GA = non-risk/heterozygous, AA = risk genotype. (**b**) Dot plot summary of qPCR data showing the overall fold change in *CACNA1C* mRNA expression by genotype. Each point represents an individual experiment (~10 cells). Numbers in brackets indicate total number of experiments per genotype. Differences between genotypes were assessed using one-way ANOVA ($F = 15.65$, $p < 0.0001$) post-hoc Tukey's multiple comparisons test. All data were recorded 28 days after induction. Data shown are mean ± s.e.m. $^{**}p < 0.01$, $^{***}p < 0.001$, $^{****}p < 0.00001$.

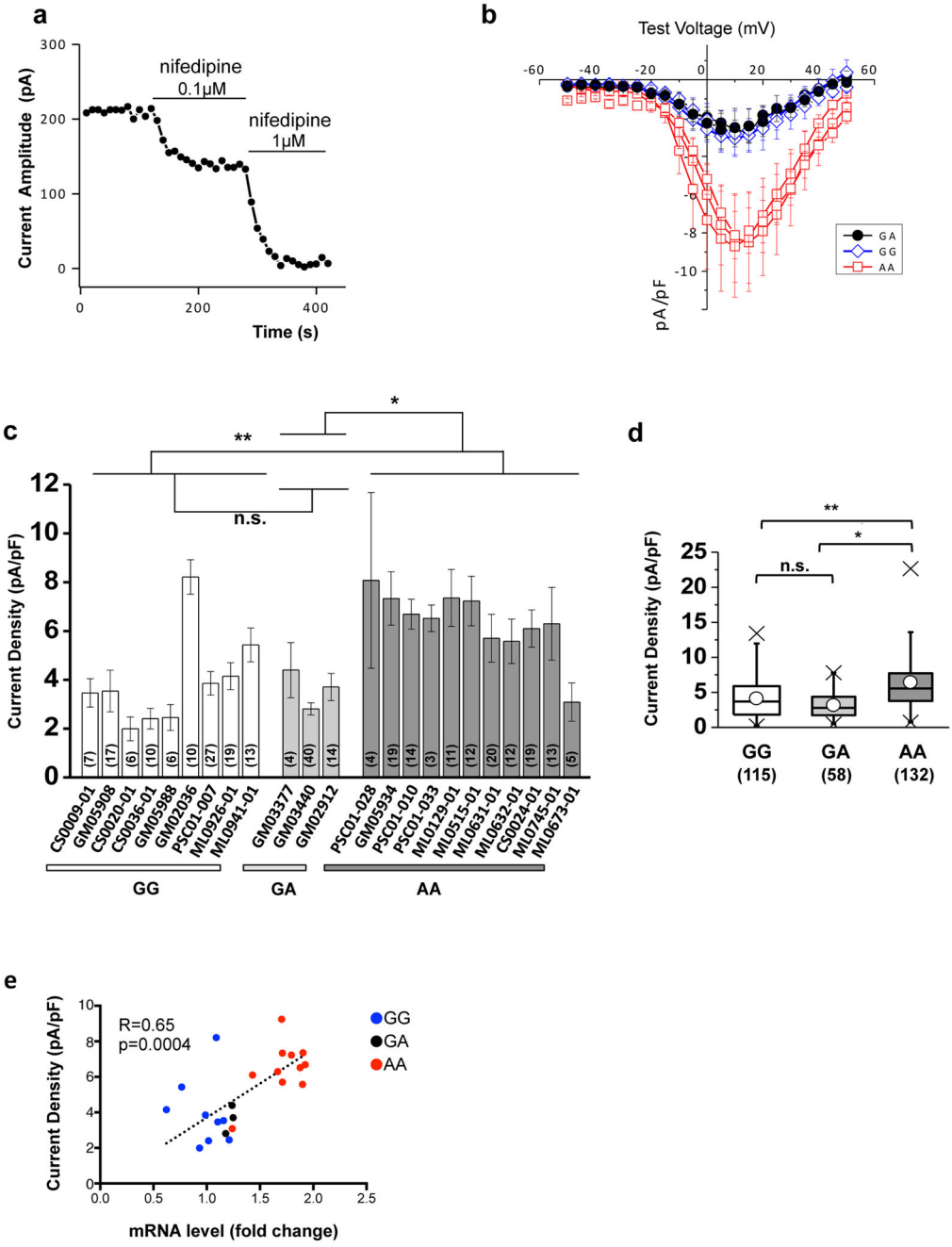

Figure 3. iNs express L-type voltage gated calcium channels measured by whole-cell patch clamp recordings

(a) Nifedipine (nif; 0.1 and 1 μM) dose dependently inhibited the voltage-gated calcium currents in iNs. **(b)** Voltage-dependent activation profile of calcium currents in induced neurons: two lines heterozygous for rs1006737 (GA, black closed circle), two lines with homozygous risk allele (red open square), and three lines with homozygous harboring non-risk allele (blue open diamond). Calcium current density was plotted against the test membrane potentials, and calculated by normalizing current amplitude (pA) of each cell to its capacitance (pF) at each voltage tested. **(c)** Voltage-gated calcium density differs among

iNs with distinct genotypes at rs1006763 within *CACNA1C*. Data shown are mean ± s.e.m. Each column represents the mean current density for that cell line. Numbers in brackets indicate the total number of cells recorded from at least two independent inductions. Differences between genotypes were assessed using one-way ANOVA ($F = 7.449$, $p = 0.0038$) and post-hoc Tukey's multiple comparisons test. **(d)** Box plots of VGCC calcium current densities from all iNs containing AA, GA, and GG alleles at rs1006737. Box indicates the 25–75% of the data. The whiskers (×) indicate the 1.5 interquartile range (IQR), a measure of statistical dispersion or midspread. All data were recorded 15–18 days after induction. Differences between genotypes were assessed using one-way ANOVA ($F = 26.65$, $p < 0.0001$) and post-hoc Tukey's multiple comparisons test. (**e)** Scatter plot of the measured current density *vs*. qPCR quantification of the 24 induced neuronal lines. Pearson correlation coefficient was calculated between the qPCR quantification and the average current density of each induced neuronal line. $^{**}p < 0.01$, $^{***}p < 0.001$, $^{****}p < 0.00001$.